Bis-Salicylaldiminato Complexes of Zinc. Examination of the Catalyzed Epoxide/CO_2 Copolymerization

Donald J. Darensbourg,* Patrick Rainey, and Jason Yarbrough

Department of Chemistry, Texas A&M University, P.O. Box 30012, College Station, Texas 77842

Received June 14, 2000

A series of salicylaldimine ligands of the general formula ($NR^2C_7H_{5-x}(R^1)_xOH$) [$x = 1$ or 2; R^1 = Me, ^{t}Bu, Cl, OMe; R^2 = 2,6-^{i}Pr$_2$C$_6$H$_3$, or 3,5-$(CF_3)_2C_6H_3$] have been synthesized and characterized via ^{1}H and ^{13}C NMR, elemental analysis, and X-ray crystallography. The concomitant series of zinc bis(salicylaldiminato) complexes of the general formula $(NR^2C_7H_{5-x}(R^1)_xO)_2Zn$ have been synthesized and characterized in the solid state by X-ray crystallography. All complexes crystallized as four coordinate monomers with distorted tetrahedral geometry about the zinc center. The O−Zn−O angles range between 105 and 112.5°, and the N−Zn−N bond angles were more obtuse spanning the range 122.9−128.9°. The only deviation from distorted tetrahedral geometry occurred when R^2 = 3,5-$(CF_3)_2C_6H_3$ which crystallized as a distorted trigonal bipyramidal dimeric species with O_{ax}−Zn−O_{ax} bond angles of 165.00(15)°. The equatorial angles approach 120° except for the N_{eq}−Zn−N_{eq} angle of 110.54(16)° which is attributed to the strain of the bridging ligands. The zinc bis(salicylaldiminato) complexes showed varying activities as catalyst precursors for the copolymerization of CO_2 and cyclohexene oxide. Activation is proposed to occur via CO_2 insertion in the phenolic Zn−O bond with simultaneous ring-opening resulting in a site for epoxide binding. The difference in activity has been ascribed to the different steric/electronic effects provided by the R^1 and R^2 substituents on the various steps of the copolymerization mechanism. The activity of the zinc bis(salicyaldiminato) catalyst precursors (<16 g·polym/g·Zn/hr) were similar to the activities of the previously reported zinc phenoxide complexes for this reaction; however, unlike the zinc phenoxide catalysts, the zinc bis(salicylaldiminato) complexes produced poly(cyclohexane carbonate) with greater than 99% carbonate linkages.

Introduction

Recently, much of our attention has been directed at the syntheses and characterization (both in solution and the solid-state) of monomeric zinc derivatives.[1,2] These efforts are motivated by the desire to uncover effective catalysts for the coupling of carbon dioxide with a wide range of epoxides.[3,4] In this report we wish to describe the preparation and solid-state structures of a variety of zinc complexes derived from the ligand, salicylaldimine. A specific example of one such cognate is illustrated in **I**. These ligands are particularly attractive because of their ease of preparation, which readily allows for varying their steric and electronic properties.[5] Indeed, Grubbs and co-workers have a short while ago exploited these monoanionic chelating salicylaldimine ligands in the synthesis of a series of nickel(II) complexes which were shown to catalyze the polymerization of ethylene at low pressures and temperatures.[6] On the basis of the closely related studies of Coates and co-workers, complexes of the type (salicylaldiminato)Zn(OR), where R = Me or COMe, should possess the capability to serve as excellent catalysts for the copolymerization of CO_2 and epoxides.[7]

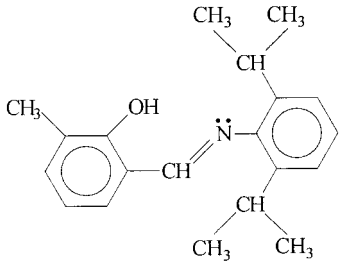

I

Herein, we divulge the synthesis and characterization of a group of bis-salicylaldiminato complexes of zinc which exhibit significant steric and electronic diversity. Included in this writing are the X-ray structures of several of the protonated ligand precursors, as well as of the zinc complexes. Thus far we have been unsuccessful in synthesizing the desired 1:1 complexes. However, these bis(salicylaldiminato)zinc derivatives have been found to display catalytic activity for the alternating copolymerization of CO_2 and cyclohexene oxide.

Experimental Section

Methods and Materials. Unless otherwise specified, all syntheses and manipulations were carried out on a double manifold Schlenk vacuum line under an atmosphere of argon or in an argon filled glovebox. Glassware was flamed out thoroughly prior to use. Toluene, tetrahydrofuran, diethyl ether, and pentane were freshly distilled from

(1) Darensbourg, D. J.; Holtcamp, M. W.; Struck, G. E.; Zimmer, M. S.; Niezgoda, S. A.; Rainey, P.; Robertson, J. B.; Draper, J. D.; Reibenspies, J. H *J. Am. Chem. Soc.* **1999**, *121*, 107.
(2) Darensbourg, D. J.; Zimmer, M. S.; Rainey, P.; Larkins, D. L. *Inorg. Chem.* **2000**, *39*, 1578.
(3) Rokicki, A.; Kuran, W. *J. Macromol. Sci., Rev. Macromol. Chem.* **1981**, *C21*, 135.
(4) Beckman, E. *Science* **1999**, *283*, 946.
(5) Grubbs, R. H. *Science* **2000**, *287*, 460.
(6) Wang, C.; Friedrich, S.; Younkin, T. R.; Li, R. T.; Grubbs, R. H.; Bansleben, D. A.; Day, M. W. *Organometallics* **1998**, *17*, 3149.
(7) Cheng, M.; Lobkovsky, E. B.; Coates, G. W. *J. Am. Chem. Soc.* **1998**, *120*, 11018.

10.1021/ic0006403 CCC: $20.00
Published on Web 01/27/2001

sodium benzophenone. 3,5-Dichlorosalicylaldehyde, 3,5-di-*tert*-butyl-2-hydroxybenzaldehyde, 2-hydroxy-5-methyl-benzaldehyde, 2-hydroxy-5-methoxy-benzaldehyde, and 2,5-(trifluoro)methylaniline were all purchased from Aldrich and used as received. 2,6-Di-isopropylaniline (90% tech) was purchased from Aldrich and was distilled under vacuum (4 mm Hg) onto molecular sieves prior to use. Bone dry carbon dioxide supplied in a high-pressure cylinder equipped with a liquid dip-tube was purchased from Scott Specialty Gases. ^{1}H and ^{13}C NMR spectra were acquired on Unity+ 300 MHz and VXR 300 MHz superconducting NMR spectrometers. The operating frequency for ^{13}C experiments was 75.41 MHz for the 300 MHz instruments. Infrared spectra were recorded on a Mattson 6021 FT-IR spectrometer with DTGS and MCT detectors. Analytical elemental analyses services were provided by Canadian Microanalytical Services Ltd.

General Procedure for the Preparation of Salicylaldimine Ligands (1a−e). The condensation of salicyaldehydes with aromatic amines was carried out by refluxing the two reactants in ethyl alcohol (100%) over molecular sieves for 2 h. Upon cooling the resulting reaction solution to 0 °C, yellow crystals precipitated from solution except in the case of **1b**, vide infra. The solid product was filtered and washed with cold ethanol and then dried in vacuo to give the desired salicylaldimine ligand in excellent yields. Any modifications are described below for each reaction.

Synthesis of $C_{20}H_{25}NO$, 1a. Upon refluxing 2-hydroxy-5-methyl-benzaldehyde (2.50 g, 18.4 mmol) and 2,6-diisopropylaniline (3.26 g, 18.4 mmol) in 30 mL of ethanol (100%) over molecular sieves afforded 4.8 g (93% yield) of the title compound as yellow crystals. A drop of trifluoroacetic acid was used to accelerate the condensation reaction. ^{1}H NMR (C_6D_6 solvent 298 K) δ 1.05 (d, 12H, CH(CH_3)$_2$), 2.34 (s, 3H, 3-CH_3), 3.01 (sept, 2H, CH(CH$_3$)$_2$), 6.7 (t, 1H, aryl), 6.9 (d, 1H, aryl), 7.03 (d, 1H, aryl), 7.1 (s, 2H, aryl), 7.96 (s, 1H, ketimine CH), 13.2 (s, 1H, OH). ^{13}C NMR (C_6D_6 solvent 298 K) δ 16.2 (3-*C*H$_3$), 24.3 (CH(*C*H$_3$)$_2$), 29.0 (*C*H(CH$_3$)$_2$), 119.4, 124.6, 126.2, 131.2, 134.7, 139.4, 147.9 (aryl), 160.7 (phenolic *ipso-C*), 167.9 (ketimine *C*). Anal. Found (calcd.): C, 81.03, (81.31); H, 8.49, (8.53); N, 4.64, (4.74). IR (ethanol) ν(CN) = 1621 cm^{-1}.

Synthesis of $C_{27}H_{39}NO$, 1b. 2-Hydroxy-3,5-di-*tert*-butylbenzaldehyde (1.5 g, 6.4 mmol) and 2,6-diisopropylaniline (1.1 g, 6.4 mmol) in 30 mL of refluxing ethanol (100%) over molecular sieves produced an oily, yellow residue. This oily product was miscible with pentane. A drop of trifluoroacetic acid was used to accelerate the condensation reaction. Separation of the title compound was achieved using a silica gel column leading to a bright yellow solid after removal of pentane 1.9 g (76% yield). IR ν(CN) = 1623 cm^{-1}. ^{1}H NMR (C_6D_6 solvent 298 K) δ 1.24 (d, 12H, CH(CH_3)$_2$), 1.40 (s, 9H, (C(CH_3)$_3$), 1.56 (s, 9H, C(CH_3)$_3$), 3.12 (sept, 2H, CH(CH$_3$)$_2$), 7.21 (m, 2H, aryl), 7.32 (s, 1H, aryl), 7.60 (d, 2H, aryl), 8.35 (s, 1H, ketimine-*H*), 13.24 (s, 1H, OH). ^{13}C NMR (C_6D_6 solvent 298 K) δ 23.91 (s, C(*C*H$_3$)$_3$), 28.91 (s, *C*(CH$_3$)$_3$), 30.14 (s, CH(*C*H$_3$)$_2$), 31.99 (s, C(*C*H$_3$)$_3$), 34.69 (s, *C*H(CH$_3$)$_3$), 35.89 (s, *C*(CH$_3$)$_3$), 118.96, 123.84, 126.13, 127.48, 138.15, 139.43, 141.35, 147.49 (s, aryl-*C*), 159.57 (s, phenolic *ipso-C*), 168.81 (s, ketimine-*C*). Anal. Found (calcd): C, 82.38 (82.31); H, 10.00 (9.90); N, 3.53 (3.51).

Synthesis of $C_{19}H_{21}NOCl_2$, 1c. Employing similar reaction conditions as for complex **1a** 2-hydroxy-3,5-dichloro-benzaldehyde (2.00 g, 10.5 mmol) and 2,6-diisopropylaniline (1.86 g, 10.5 mmol) were refluxed in 30 mL of ethanol (100%) for 2h. Upon cooling, the reaction solution to 0 °C afforded bright yellow crystals 3.21 g (87% yield) of **1c**. IR ν(CN) = 1624 cm^{-1}. ^{1}H NMR (C_6D_6 solvent 298 K) δ 1.01 (d, 12H, CH(CH_3)$_2$), 2.80 (sept, 2H, CH(CH$_3$)$_2$), 6.65 (s, 1H, aryl), 7.05−7.15 (m, 3H, aryl), 7.50 (s, 1H, ketimine-*H*), 14.32 (s, 1H, OH). Anal. Found (calcd): C, 64.60 (65.15); H, 5.88 (6.04).

Synthesis of $C_{20}H_{25}NO_2$, 1d. Similarly, 2-hydroxy-5-methoxy-benzaldehyde (2.50 g, 16.4 mmol) and 2,6-diisopropylaniline (2.91 g, 16.4 mmol) refluxed in 30 mL of ethanol provided 4.2 g (82% yield) of bright yellow crystals upon cooling the reaction solution to 0 °C. IR ν(CN) = 1629 cm^{-1}. ^{1}H NMR (C_6D_6 solvent 298 K) δ 1.06 (d, 12H, CH(CH_3)$_2$), 3.00 (sept, 1H CH(CH$_3$)$_2$), 3.27 (s, 3H, OCH_3), 6.61 (d, 1H, aryl), 6.78 (dd, 1H, aryl), 7.04 (s) 7.10 (s, 4H, aryl), 7.85 (s, 1H, ketimine-*H*), 12.72 (s, 1H, OH). Anal. Found (calcd): C, 76.99 (77.14); H, 8.07 (8.09), N, 4.35 (4.50).

Synthesis of $C_{16}H_{11}NOF_6$, 1e. 2-Hydroxy-3-methyl-benzaldehyde (1.1 g, 8.4 mmol) and 3,5-(trifluoro)methyl-aniline (1.9 g, 8.4 mmol) in 30 mL of ethanol were refluxed for 2 h to afford 2.2 g (76% yield) of the title compound as yellow crystals when the reaction solution was cooled to 0 °C. IR ν(CN) = 1614 cm^{-1}. ^{1}H NMR (C_6D_6 solvent 298 K) δ 2.28 (s, 3H, CH_3), 6.65 (t, 1H, aryl), 6.75 (d, 1H, aryl), 6.91 (d, 1H, aryl), 7.01 (s, 1H, aryl), 7.13 (s, 2H, aryl), 7.56 (s, 1H, ketimine-*H*), 12.31 (s, 1H, O*H*).

Synthesis of Zn($C_{20}H_{24}NO$)[N(Si(CH$_3$)$_3$)$_2$], 2a. A 5 mL yellow solution of complex **1a** (0.15 g, 0.52 mmol) in THF was added via cannula to a 5 mL colorless solution of Zn[N(Si(CH$_3$)$_3$)$_2$]$_2$ (0.20 g, 0.52 mmol) dissolved in THF. The color of the solution changed to chartreuse immediately upon addition of **1a** to the zinc amide solution. The reaction solution was allowed to stir at ambient temperature for 2h. All volatiles were removed via vacuum to produce a yellow powder 0.24 g, (87% yield). ^{1}H NMR (C_6D_6 solvent 298 K) δ 0.28 (s, 18H, N(Si(CH_3)$_3$)$_2$), 0.97 (d, 6H, CH(CH_3)$_2$), 1.29 (d, 6H, CH(CH_3)$_2$), 1.39 (m, THF), 2.45 (s, 3H, CH_3), 3.05 (sept, 2H, CH(CH$_3$)$_2$), 3.61 (m, THF), 6.50−7.11 (m, 6H, aryl), 7.84 (s, 1H, ketimine-*H*). Anal. Found (calcd): C, 59.48 (60.03); H, 8.02 (8.14); N, 5.17 (5.39).

Synthesis of Zn($C_{27}H_{38}NO$)[N(Si(CH$_3$)$_3$)$_2$], 2b. A 5 mL yellow, THF solution of complex **1b** (0.10 g, 0.25 mmol) was added via cannula to a 5 mL THF solution of Zn[N(Si(CH$_3$)$_3$)$_2$]$_2$ (0.10 g, 0.25 mmol). The solution color changed to chartreuse immediately upon addition of **1b** to the zinc amide solution. All volatiles were removed via vacuum to produce a yellow powder 0.13 g, (81% yield). ^{1}H NMR (C_6D_6 solvent 298 K) δ 0.90 (d, 6H, CH(CH_3)$_2$), 1.22 (d, 6H, CH(CH_3)$_2$), 1.29 (s, 9H, C(CH_3)$_3$), 1.36 (m, THF), 1.71 (s, 9H, C(CH_3)$_3$), 2.99 (sept, 2H, CH(CH$_3$)$_2$), 3.57 (m, THF), 6.85 (d, 1H, aryl), 7.06 (m, 3H, aryl), 7.78 (d, 1H, aryl), 7.97 (s, 1H, ketimine-*H*). Anal. Found (calcd): C, 63.72 (64.10); H, 9.02(9.13); N, 4.45(4.53).

Synthesis of Zn($C_{20}H_{24}NO$)(CH_2CH_3), 3a. Complex **1a** (0.38 g, 1.3 mmol) was dissolved in 5 mL of hexane to give a yellow-orange solution. This solution was then cannulated onto a 10 mL colorless solution of a Zn(CH_2CH_3)$_2$ (0.79 g, 6.4 mmol) in hexane to give a chartreuse solution which was allowed to stir for 2 h. Evacuation of all volatiles afforded a yellow powder 0.33 g (65% yield). ^{1}H NMR (C_6D_6 solvent 298 K) δ 0.45 (quart., 2H CH_2CH$_3$), 1.03 (d, 6H, CH(CH_3)$_2$), 1.20 (t, 3H, CH$_2$CH_3), 1.33 (d, 6H, CH(CH_3)$_2$), 1.88 (s, 3H, CH$_3$), 3.42 (br, 2H, CH(CH$_3$)$_2$), 6.49 (t, 1H, aryl), 6.72 (dd, 1H, aryl), 6.93 (d, 1H, aryl), 7.13 (m, 3H, aryl), 7.94 (s, 1H, ketimine-*H*).

Synthesis of Zn($C_{27}H_{38}NO$)(CH_2CH_3), 3b. Complex **1b** (0.30 g, 0.76 mmol) was dissolved in 5 mL of hexane to give a yellow solution which was added to a 10 mL colorless solution of Zn(CH_2CH_3)$_2$ (0.47 g, 3.8 mmol) in hexane to produce a chartreuse solution. Evacuation of all volatiles afforded a yellow powder 0.28 g (76% yield). ^{1}H NMR (C_6D_6 solvent 298 K) δ 0.40 (quart., 2H, CH_2CH$_3$), 0.90 (d, 6H, CH(CH_3)$_2$), 1.196 (s, 18H, C(CH_3)), 1.23 (t, 3H, CH$_2$CH_3), 1.62 (s, 18H, C(CH_3)), 2.83 (sept, 2H, CH(CH$_3$)$_2$), 6.85 (d, 1H, aryl), 7.05 (m, 3H, aryl), 7.79 (d, 1H, aryl), 7.95 (s, 1H, ketimine-*H*).

Synthesis of Zn($C_{20}H_{24}NO$)$_2$, 4a. Complex **1a** (0.31 g, 1.0 mmol) was dissolved in 5 mL of pentane to give a yellow solution. This solution was added via cannula onto a clear and colorless solution of Zn[N(Si(CH$_3$)$_3$)$_2$]$_2$ (0.20 g, 0.50 mmol) in pentane to afford a chartreuse solution. The reaction was allowed to stir for 1.5 h after which all volatiles were removed via vacuum to give a bright yellow powder 0.30 g (89% yield). Complex **4a** could be further purified by recrystallization as described in the experimental X-ray structural studies section. ^{1}H NMR (C_6D_6 solvent 298 K) δ 0.81 (d, 12H, CH(CH_3)$_2$), 1.01 (d, 12H, CH(CH_3)$_2$), 2.21 (s, 6H, CH_3), 3.23 (br, 4H, CH(CH$_3$)$_2$), 6.42 (t, 2H, aryl), 6.7 (dd, 2H, aryl), 6.95−7.10 (m, 8H, aryl), 7.83 (s, 2H, ketimine-*H*). ^{13}C NMR (C_6D_6 solvent 298 K) δ 23.42 (s, *C*H$_3$), 25.34 (s, CH(*C*H$_3$)$_2$), 28.83 (s, *C*H(CH$_3$)$_2$), 114.87, 117.41, 124.57, 127.10, 128.39, 128.71, 132.45, 134.70, 136.66, 142.25, 147.38 (s, *aryl-C*), 172.23 (s, phenolic *ipso-C*), 175.36 (s, ketimine-*C*). Anal. Found (calcd): C, 72.09 (73.44); H, 7.25 (7.40); N, 4.12 (4.28).

Synthesis of Zn($C_{27}H_{38}NO$)$_2$, 4b. Complex **1b** (0.20 g, 0.50 mmol) dissolved in 5 mL of THF to give a yellow solution was added via cannula onto a colorless 5 mL THF solution of Zn[N(Si(CH$_3$)$_3$)$_2$]$_2$ (0.10 g, 0.25 mmol) to produce a chartreuse solution. Evacuation of all volatiles afforded 0.18 g (85% yield) of a bright yellow powder.

Complex **4b** could be further purified by recrystallization as described in the experimental X-ray structural studies section. ^{1}H NMR (C_6D_6 solvent 298 K) δ 0.90 (d, 6H, CH(CH_3)$_2$), 1.19 (s, 18H, CH(CH_3)$_2$), 1.22 (d, 18H, C(CH_3)$_3$), 1.62 (s, 18H, C(CH_3)$_3$), 2.63 (sept, 2H, CH(CH$_3$)$_2$), 3.94 (sept, 2H, CH(CH$_3$)$_2$), 6.73 (d, 2H, aryl), 6.92 (m, 2H, aryl), 7.00−7.04 (m, 4H, aryl), 7.65 (d, 2H, aryl), 7.85 (s, 2H, ketimine-*H*). ^{13}C NMR (C_6D_6 solvent 298 K) δ 23.12, 24.12, 25.40, 28.45, 28.92 (s, CH(*C*H$_3$)$_2$), 30.44, 31.78 (s, *C*(CH$_3$)$_3$), 34.30, 36.25 (s, *C*(CH$_3$)$_3$), 117.58, 124.53, 127.38, 130.70, 132.02, 136.05, 142.47, 147.94 (s, *aryl*), 171.73 (s, phenolic *ipso-C*), 176.62 (s, ketimine-*C*). Anal. Found (calcd): C, 75.61 (76.25); H, 9.21 (9.01).

Synthesis of Zn(C$_{19}$H$_{20}$NOCl$_2$)$_2$, 4c. Complex **1c** (0.18 g, 0.52 mmol) was dissolved in 5 mL of pentane to give a yellow-orange solution followed by cannulation to a 10 mL pentane solution of Zn[N(Si(CH$_3$)$_3$)$_2$]$_2$ (0.10 g, 0.26 mmol) to afford an immediate yellow precipitate. The precipitate was filtered onto a glass frit and washed with 3 washings of 5 mL of pentane each to give 0.19 g (94% yield) yellow solid. Complex **4c** could be further purified by recrystallization as described in the experimental X-ray structural studies section. ^{1}H NMR (C_6D_6 solvent 298 K) δ 0.71 (br, 12H, CH(CH_3)$_2$), 0.97 (d, 12H CH(CH_3)$_2$), 3.1 (br, 4H, CH(CH$_3$)$_2$), 6.37 (d, 2H, aryl), 6.87−7.00 (m, 6H, aryl), 7.26 (d, 1H, aryl), 7.30 (s, 2H, ketimine-*H*). ^{13}C NMR (C_6D_6 solvent 298 K) δ 23.49, 25.18, 28.77 (s, *C*H(*C*H$_3$)$_2$), 118.65, 124.88, 133.81, 136.02, 142.02, 146.35 (*aryl-C*), 165.98 (s, phenolic *ipso-C*), 174.59 (s, ketimine-*C*). Anal. Found (calcd): C, 59.45 (59.74); H, 5.20 (5.28).

Synthesis of Zn(C$_{20}$H$_{24}$NO$_2$)$_2$, 4d. Complex **1d** (0.49 g, 1.6 mmol) was dissolved in 10 mL of THF to give a yellow-orange solution followed by cannulation onto a 10 mL THF solution of Zn[N(Si(CH$_3$)$_3$)$_2$]$_2$ (0.30 g, 0.78 mmol) to give a chartreuse solution. Evacuation of all volatiles produced a sticky yellow solid that was washed several times with pentane to provide a yellow powder 0.47 g (87% yield). Complex **4d** could be further purified by recrystallization as described in the experimental X-ray structural studies section. ^{1}H NMR (C_6D_6 solvent 298 K) δ 0.85 (d, 6H, CH(CH_3)$_2$), 1.04 (d, 18H, CH(CH_3)$_2$), 3.29 (s, 10H, OCH_3 peak conceals smaller intensity signal of CH(CH$_3$)$_2$ septet), 6.19 (s, 2H, aryl), 7.00 (s, 10H, aryl), 7.68 (s, 2H, ketimine-*H*). ^{13}C NMR (C_6D_6 solvent 298 K) δ 23.20, 25.43, 29.72 (*C*H(*C*H$_3$)$_2$), 56.37 (s, O*C*H$_3$), 116.82, 122.33, 127.69, 142.71, 147.36, 150.42 (*aryl-C*), 169.34 (phenolic *ipso-C*), 174.38 (s, ketimine-*C*). Anal. Found (calcd): C, 68.05 (70.01); H, 6.98 (7.05); N, 3.67 (4.08).

Synthesis of Zn(C$_{16}$H$_{10}$NOF$_6$)$_2$, 4e. Complex **1e** (0.45 g, 1.3 mmol) was dissolved in 10 mL of pentane to give a yellow solution followed by cannulation onto a 10 mL pentane solution of Zn[N(Si(CH$_3$)$_3$)$_2$]$_2$ (0.25 g, 0.65 mmol) to afford an immediate yellow precipitate. The precipitate was filtered onto a glass frit and washed with 3 washings of 5 mL each of pentane to give a yellow solid 0.45 g (92% yield). Complex **4e** could be further purified by recrystallization as described in the experimental X-ray structural studies section. ^{1}H NMR (C_6D_6 solvent, 298 K) δ 2.36 (s, 6H, CH_3), 6.41 (t, 2H, aryl), 6.52 (d, 2H, aryl), 6.82 (d, 2H, aryl), 7.01 (d, 2H, aryl), 7.53 (s, 2H, aryl), 7.69 (s, 2H, ketimine-*H*).

Attempted Syntheses of (Salicyaldiminato)Zn(OR) (R = Me, Ph, or COMe) Derivatives. As mentioned earlier, the synthesis of mono-salicylaldiminato zinc complexes has not yet been accomplished. The first attempts at making these complexes were modeled after Coates' synthesis of the highly active diimine zinc acetate catalysts wherein the sodium or lithium salt of the salicylaldimine ligand was reacted with Zn(OAc)$_2$. Typically, the sodium or lithium salt was dissolved in 30 mL of THF and allowed to slowly drop onto a 5 equiv excess of Zn(OAc)$_2$ in 30 mL of THF overnight. After a 12 h reaction time, the slurry was filtered over a glass frit and the chartreuse solution taken to dryness under vacuum. Analysis of the product by ^{1}H NMR showed that the bis-salicylaldiminato zinc complexes were produced as opposed to the targeted (salicylaldiminato)Zn(OAc) complexes, regardless of which salicylaldimine ligand was used as the starting material. Similar reaction procedures were used with various zinc starting materials such as ZnCl$_2$ dissolved in THF, Zn(OTf)$_2$ dissolved in acetonitrile, and Zn(CH$_3$CN)$_4$(BF$_4$)$_2$ dissolved in acetonitrile with similar results. In other words, when soluble zinc starting materials were used in excess, the bis ligand complexes were produced. Evidently, the salicylaldiminato ligands are not sterically bulky enough to inhibit the formation of bis ligand species. Another route that was pursued in the attempted formation of mono-salicylaldiminato complexes was through the reaction of methanol, stoichiometric amounts and in excess, or 1 equiv of a 2,6-di-substituted phenol with the (salicylaldiminato)Zn(R) (R = Et or N(Si(Me)$_3$)$_2$) complexes **2** and **3** in THF. These solutions were allowed to stir at ambient temperature from 1.5 to 12 h after the addition of protic reagent. In all cases, analysis by NMR showed bis ligand products or a complex mixture of products whose identity could not be determined.

Table 1. Crystallographic Data for Complexes **1a**, **1c**, and **1e**

	1a	**1c**	**1e**
empirical formula	$C_{20}H_{26}NO$	$C_{19}H_{21}Cl_2NO$	$C_{16}H_{11}F_6NO$
fw	296.42	350.27	347.26
crystal system	orthorhombic	monoclinic	orthorhombic
space group	$P2_12_12_1$	$P(1)/n$	$P2_12_12_1$
V, Å^3	1720.6(11)	3665.1(5)	1474.5(3)
Z	4	4	4
a, Å	7.541(3)	11.1221(8)	5.0563(6)
b, Å	9.580(4)	14.6595(11)	12.8168(15)
c, Å	23.817(9)	22.4799(16)	22.753(3)
α, deg	90	90	90
β, deg	90	90.475(2)	90
γ, deg	90	90	90
T, K	110(2)	110(2)	110(2)
d(calcd), g/cm^3	1.144	1.270	1.564
absorp coeff, mm^{-1}	0.069	0.716	0.150
R,[a] %	4.91	6.75	3.69
R$_w$,[a] %	12.97	15.91	11.13

[a] $R = \sum||F_o| - |F_c||/\sum F_o$. $Rw = \{[\sum w(F_o^2 - F_c^2)^2/[\sum w(F_o^2)^2]\}^{1/2}$.

X-ray Structural Studies. Complexes 1a, 1c, 1e, and 4a−4e. Single crystals suitable for X-ray analysis were obtained for complexes **1a, 1c, 1e,** and **4a−4e** by dissolving each complex in a minimal amount of diethyl ether inside a test tube, which was contained inside a Schlenk tube with approximately 5 mL of toluene under an atmosphere of argon. The diethyl ether was allowed to slowly evaporate into the toluene solvent by keeping the tube at 0 °C overnight. Crystal data and details of data collection for complexes **1a**, **1c**, and **1e** are provided in Table 1. The same information for complexes **4a−4e** is provided in Table 2. The X-ray data were collected on a Bruker CCD diffractometer and covered more than a hemisphere of reciprocal space by a combination of three sets of exposures; each exposure set had a different φ angle for the crystal orientation and each exposure covered 0.3° in ω. The crystal-to-detector distance was 4.9 cm. Crystal decay was monitored by repeating the data collection for 50 initial frames at the end of the data set and analyzing the duplicate reflections; crystal decay was negligible. The space group was determined based on systematic absences and intensity statistics.[8] The structure was solved by direct methods and refined by full-matrix least-squares techniques. All non-H atoms were refined with anisotropic displacement parameters. All H atoms attached to C atoms were placed in idealized positions and refined using a riding model with aromatic C−H = 0.96 Å, methyl C−H = 0.98 Å, and with fixed isotropic displacement parameters equal to 1.2 (1.5 for methyl H atoms) times the equivalent isotropic displacement parameter of the atom to which they were attached. The methyl groups were allowed to rotate about their local 3-fold axis during refinement.

For all complexes, data collection, and cell refinement, SMART;[8] data reduction, SAINTPLUS (Bruker[9]); program(s) used to solve structures, *SHELXS-86* (Sheldrick[10]); program(s) used to refine structures, *SHELXL-97* (Sheldrick[11]); molecular graphics, *SHELXTL-Plus*

(8) *SMART 1000 CCD*; Bruker Analytical X-ray Systems: Madison, WI, 1999.
(9) *SAINT-Plus*, version 6.02; Bruker Analytical X-ray Systems: Madison, WI, 1999.
(10) Sheldrick, G. *SHELXS-86 Program for Crystal Structure Solution*; Institut fur Anorganische Chemie der Universitat: Gottingen, Germany, 1986.
(11) Sheldrick, G. *SHELXL-97 Program for Crystal Structure Refinement*; Institut fur Anorganische Chemie der Universitat: Gottingen, Germany, 1997.

Table 2. Crystallographic Data for Complexes **4a**, **4b**, **4c**, **4d**, and **4e**

	4a	4b	4c	4d	4e
empirical formula	$C_{40}H_{50}N_2O_2Zn$	$C_{54}H_{76}N_2O_2Zn\cdot 3PhMe$	$C_{38}H_{40}Cl_4N_2O_2Zn$	$C_{40}H_{48}N_2O_4Zn$	$C_{64}H_{44}F_{24}N_4O_4Zn_2\cdot PhMe$
fw	656.19	1126.94	763.94	654.21	1611.94
crystal system	monoclinic	triclinic	monoclinic	monoclinic	monoclinic
space group	$P2_1/n$	$P\bar{1}$	$C2/c$	$P2_1/n$	$P2/n$
V, Å^3	3504.0(7)	3333.4(5)	7227.2(1)	3602.6(9)	3672.8(5)
Z	4	4	8	4	2
a, Å	10.3771(13)	14.3993(13)	19.7086(16)	12.0222(17)	13.6459(10)
b, Å	17.444(2)	15.3231(13)	17.3307(14)	14.924(2)	16.6239(13)
c, Å	19.524(2)	15.8728(14)	22.5847(18)	20.888(3)	16.9673(13)
α, deg	90	89.257(2)	90	90	90
β, deg	97.494(2)	73.296(2)	110.4660(10)	105.989(3)	107.402(2)
γ, deg	90	83.682(2)	90	90	90
T, K	110(2)	110(2)	110(2)	110(2)	110(2)
d(calcd), g/cm^3	1.244	1.614	1.492	1.309	1.523
absorp coeff, mm^{-1}	0.737	0.826	1.017	0.726	0.767
R,[a] %	6.11	7.99	6.22	6.20	7.18
R_w,[a] %	14.86	19.40	14.91	14.25	17.16

[a] $R = \sum||F_o| - |F_c||/\sum F_o$. $Rw = \{[\sum w(F_o^2 - F_c^2)^2/[\sum w(F_o^2)^2]\}^{1/2}$.

Scheme 1

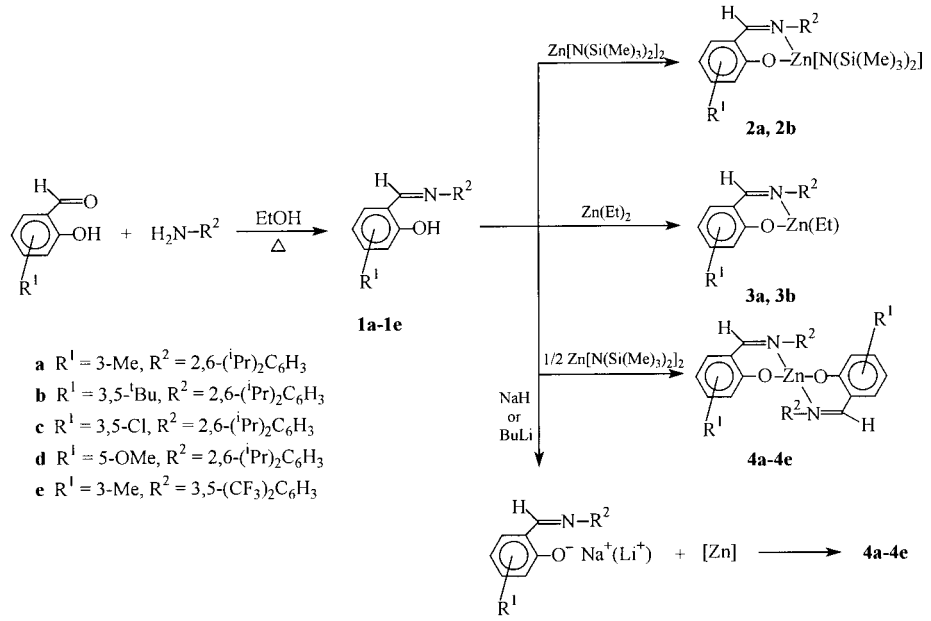

a R^1 = 3-Me, R^2 = 2,6-(^{i}Pr)$_2$C$_6$H$_3$
b R^1 = 3,5-^{t}Bu, R^2 = 2,6-(^{i}Pr)$_2$C$_6$H$_3$
c R^1 = 3,5-Cl, R^2 = 2,6-(^{i}Pr)$_2$C$_6$H$_3$
d R^1 = 5-OMe, R^2 = 2,6-(^{i}Pr)$_2$C$_6$H$_3$
e R^1 = 3-Me, R^2 = 3,5-(CF$_3$)$_2$C$_6$H$_3$

version 5.0 (Bruker[12]); software to prepare material for publication, *SHELXTL-Plus* version 5.0 (Bruker).[12]

Copolymerization of Epoxides and Carbon Dioxide. A typical copolymerization run was carried out as follows: ca. 0.2 mmol of the respective zinc bis(salicyaldiminato) complex was dissolved in 20 mL of cyclohexene oxide or propylene oxide. The solution was loaded via an injection port into a 300 mL autoclave which had previously been dried overnight under vacuum at 90 °C. The autoclave was then placed under 700−800 psi of carbon dioxide and heated to the appropriate temperature, usually 80 °C. After the allotted time (20 h), the autoclave was allowed to cool to room temperature, following which the polymer was extracted. Unreacted monomer was removed by repeated precipitation of the polymer from a dichloromethane solution with methanol.

The poly(cyclohexane carbonate) copolymers were analyzed by ^{1}H NMR, where the hydrogens adjacent to the carbonate linkages afford a signal at 4.6 ppm and the absence of polyether linkages was verified by the absence of a signal at 3.5 ppm. The rest of the aliphatic protons produce broad signals in the range of 1.2−2.2 ppm. Infrared spectroscopy was also used to verify the ν(CO) stretch for polycarbonate at 1750 cm^{-1}. The number average (Mn) and weight average (Mw) molecular weights, and concomitant the polydispersities of the copolymers, were obtained employing gel permeation chromatography in the laboratories of PAC Polymers, Inc.

Results and Discussion

The salicylaldimine ligands **1a**−**e** were easily prepared by simple condensations of salicylaldehydes with aromatic amines in the presence of the catalyst, trifluoroacetic acid, in excellent yields as outlined in Scheme 1. Compounds **1a**, **1c**, and **1e** readily crystallized from the reaction solution upon cooling to 0 °C and their characterization by X-ray diffraction was accomplished for comparison with the subsequently synthesized salicylaldiminato zinc complexes. Immediately apparent is the average C═N bond distance for **1a**, **1c**, and **1e** at 1.281[5] Å, which is correct for a C═N bond and is consistent with the IR data obtained where ν(CN) for all three complexes lies between 1620 and 1629 cm^{-1}.[13] It should be noted that the $C_{imine}-C_{phenyl}$ and $N_{imine}-C_{phenyl}$ distances are somewhat shorter than expected for the analogous single bonds (1.54 and 1.51 Å for C−C and

(12) *SHELXTL*, version 5.0; Bruker Analytical X-ray Systems: Madison, WI, 1999.

(13) Kovcic, J. E. *Spectrochim. Acta* **1967**, *23A*, 183.

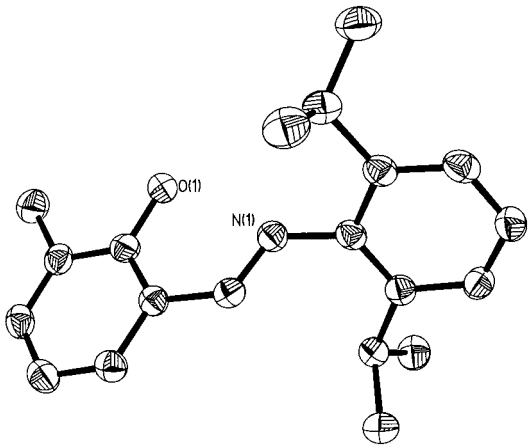

Figure 1. Thermal ellipsoid representation of compound **1a**.

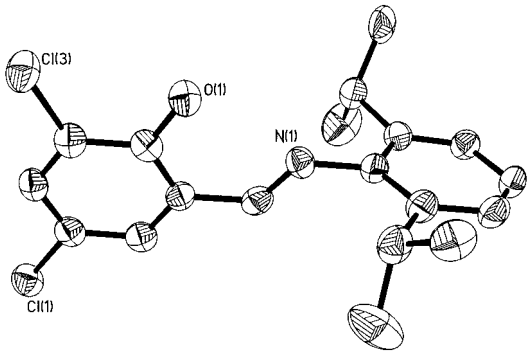

Figure 2. Thermal ellipsoid representation of compound **1c**.

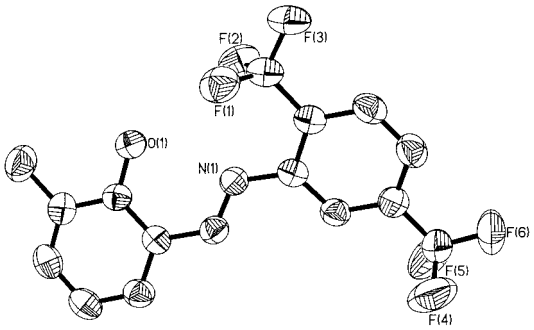

Figure 3. Thermal ellipsoid representation of compound **1e**.

C−N bonds, respectively) at an average of 1.447[7] and 1.419[6] Å, respectively. This can be attributed to partial conjugation between the imine C and N atoms and the aromatic rings. Thermal ellipsoid drawings of the neutral ligand precursors, **1a**, **1c**, and **1e**, are shown in Figures 1−3, respectively.

As mentioned previously and discussed in detail later, the synthesis of (salicylaldiminato)Zn(OR) (where R = Me, Ph, or COMe) has not yet been accomplished; however, the synthesis of mono(salicylaldiminato)ZnR (where R = Et or $[N(Si(Me)_3)_2]$) is easily achieved by reacting 1 equiv of the salicylaldimine ligand with the appropriate zinc reagent, as depicted in Scheme 1, to form complexes **2a**, **2b**, **3a**, and **3b**. Solid-state characterization of these derivatives via X-ray diffraction has not yet been accomplished due to a lack of suitable crystals of these complexes. Hence, we cannot rule out the possibility that complexes **3a**,**b** are dimers. On the other hand, because of the bulky nature of the salicylaldimine ligands and the amide group, dimer formation is unlikely in complexes **2a**,**b**. The ^{1}H NMR of complexes **2** and **3,** and the fact that both complexes are bright yellow solids whereas the starting zinc reactants in both cases are colorless liquids, support the assignment of a monoadduct species. The best evidence for this assignment is in the ^{1}H NMR chemical shifts of specific resonances on the salicylaldiminato ligand as well as the appearance of new peaks of appropriate intensities associated with the hexamethylsilylamide and ethyl functionalities on the complexes, respectively.

The ^{1}H NMR spectra in C_6D_6 solvent of complexes **2a** and **2b** exhibit large singlets at 0.28 ppm, which integrates to the appropriate 18H for the silylamide group. For **2a**, the isopropyl methyl groups appear as two doublets at 0.97 and 1.29 ppm that integrate to 6H for both doublets. In the starting salicylaldimine ligand **1a**, the isopropyl methyl groups appear as one doublet at 1.05 ppm integrating to 12H. The septet associated with the lone hydrogen on the isopropyl group for **2a** has shifted to 2.45 ppm (2H) from 3.01 ppm (2H) in **1a**. Finally, the ketimine hydrogen shifts from 7.96 ppm for **1a** to 7.84 ppm for **2a**. As discussed in the Experimental Section, similar shifts occur for the ^{1}H resonances of complexes **2b**, **3a**, and **3b** with the exception that a quartet and triplet appear in the spectra for **3** at 0.45 and 1.20 ppm corresponding to the remaining ethyl group on the zinc center in these complexes. It is noteworthy that the ^{1}H NMR spectra for the bis-salicylaldiminato zinc analogues **4a** and **4b** are completely different than that just described for the monoadducts.

The impetus for the synthesis of the mono-salicylaldiminato zinc complexes **2** and **3** was to use these readily isolated starting materials in the synthesis of three-coordinate (salicylaldiminato)-Zn(OR) complexes (where R = Me, Ph, or COMe). Once complexes **2** and **3** were isolated, it was hoped to subsequently react them with a protic reagent such as methanol, phenol, or acetic acid to protonate the amide or ethyl bases and form the desired three-coordinate compounds. Unfortunately the synthesis of (salicylaldiminato)Zn(OR) complexes proved to be nontrivial. Upon the addition of a protic reagent and workup of the products, it was discovered through ^{1}H NMR that a mixture of bis(salicylaldiminato)Zn and $Zn(OR)_2$ was produced. Evidently, a disproportionation reaction occurred to produce a stable four-coordinate zinc complex with nitrogen donors and zinc alkoxides as extended aggregates. Indeed, similar products were observed when the salicylaldimine ligands were first deprotonated with NaH or alkyllithium reagents and reacted with various zinc salts such as $Zn(OAc)_2$, $Zn(OTf)_2$, $ZnCl_2$, and $Zn(CH_3CN)_4(BF_4)_2$. These reactions are depicted schematically at the bottom of Scheme 1.

Complexes **4a**−**e** were conveniently synthesized by reacting 2 equiv of the appropriate salicylaldimine ligand with 1 equiv of zinc bis-hexamethylsilylamide in either THF or pentane. Pentane solvent resulted in a cleaner product and higher yields for the complexes that were insoluble in pentane (e.g., complexes **4c** and **4e**). All of the complexes have been crystallographically characterized, and thermal ellipsoid representations of **4a**−**e** and a simplified drawing of **4e** are given in Figures 4−8 and Figure 9, respectively. The relevant bond lengths and angles are compiled in Table 3 for **4a**−**e**. Complexes **4a**−**d** crystallized out in distorted tetrahedral geometries with O−Zn−O angles ranging between 105° and 112.5°. The N−Zn−N bond angles were typically more obtuse spanning the range 122.9−128.9° and can most probably be attributed to the larger bulk of the 2,6-$(^i Pr)_2C_6H_3$ group attached to the nitrogen atoms. Zn−O bond distances for these complexes in general are slightly longer than the Zn−O bond distances for Zn bis(phenoxides); this observation is most likely due to the fact that the phenolic group in **4a**−**d** must accommodate the chelating ring geometry. Complexes **4a**−**d** contain Zn−O bond lengths ranging between

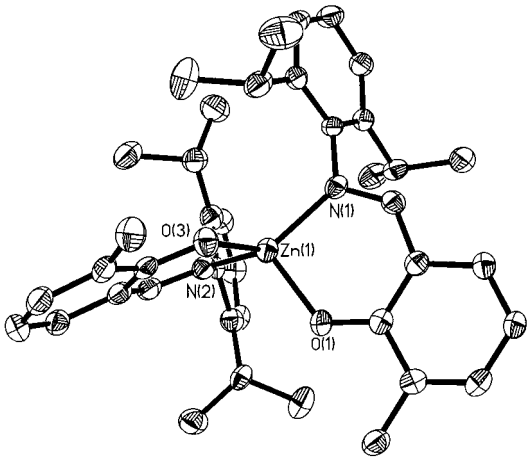

Figure 4. Thermal ellipsoid representation of $Zn(C_{20}H_{24}NO)_2$, complex **4a**.

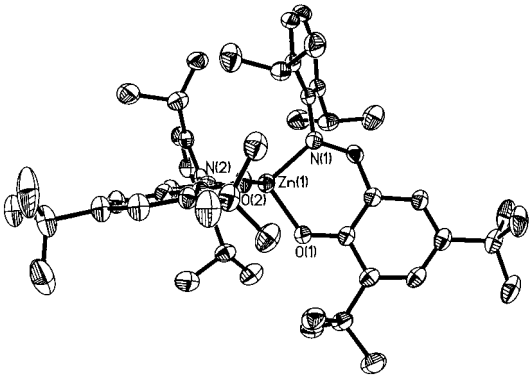

Figure 5. Thermal ellipsoid representation of $Zn(C_{27}H_{39}NO)_2$, complex **4b**.

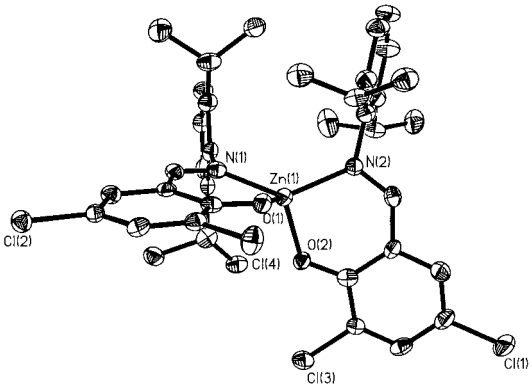

Figure 6. Thermal ellipsoid representation of $Zn(C_{19}H_{20}NOCl_2)_2$, complex **4c**.

1.908(3)−1.949(3) Å. Interestingly, the shorter bond distances are observed with more electron donating substituents on the phenol ring such as ^{t}Bu and OMe groups and the longer distances are observed with the electron withdrawing Cl groups on the phenol ring. The imine C−N bond appears to retain its double bond character once bound to the zinc center, although some lengthening outside of error occurs in the C═N bond on going from the free ligand to the bound ligand as a result of the possibility of increased resonance throughout the six-membered chelating ring. The double bond character of the imine functionality is exemplified in the average Zn−N bond distances for complexes **4a**−**d** being 1.999[9], which suggests primarily electron donation from the nitrogen lone pair to the zinc center.

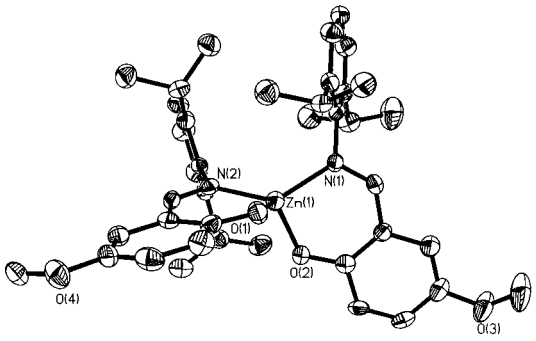

Figure 7. Thermal ellipsoid representation of $Zn(C_{20}H_{24}NO_2)_2$, complex **4d**.

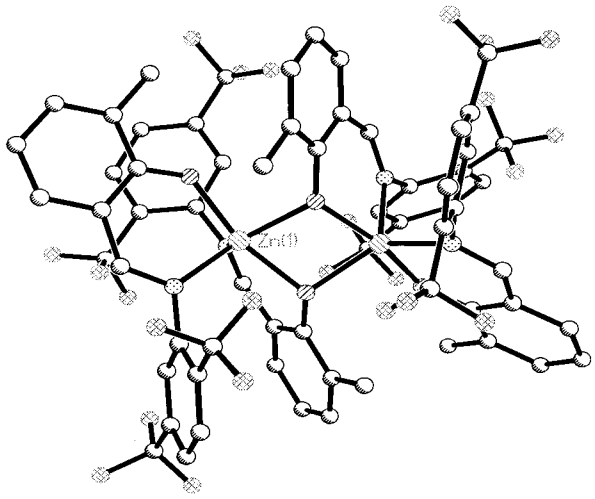

Figure 8. Thermal ellipsoid representation of $Zn(C_{16}H_{11}NOF_6)_2$, complex **4e**.

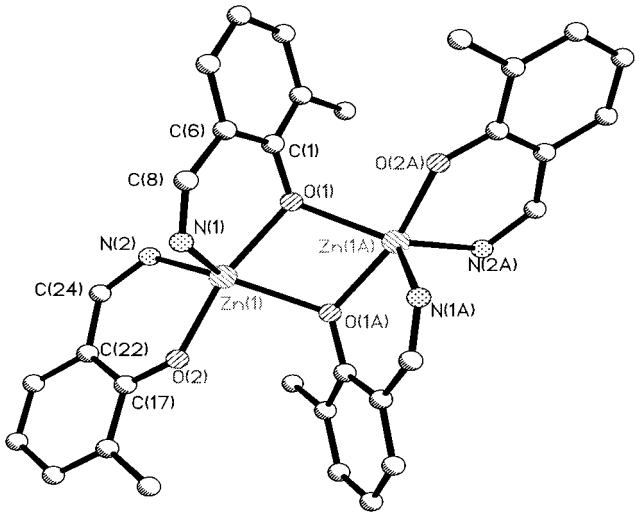

Figure 9. Simplified ball-and-stick drawing of complex **4e**.

While complexes **4a**−**d** in the solid-state adapted distorted tetrahedral monomeric structures, complex **4e** was found to be a dimer with bridging salicylaldiminato ligands resulting in a distorted trigonal bipyramidal geometry around each zinc center. This result is likely due to the decreased steric bulk of the aromatic ring attached to the nitrogen rather than electronic effects of the CF_3 groups. The chelating salicylaldiminato ligand on the zinc center of this dimeric species contains bond lengths similar to those observed for the other derivatives **4a**−**d** (see Table 3). As would be expected, the bond lengths for the bridging ligands, specifically the Zn−O and Zn−N distances,

Scheme 2

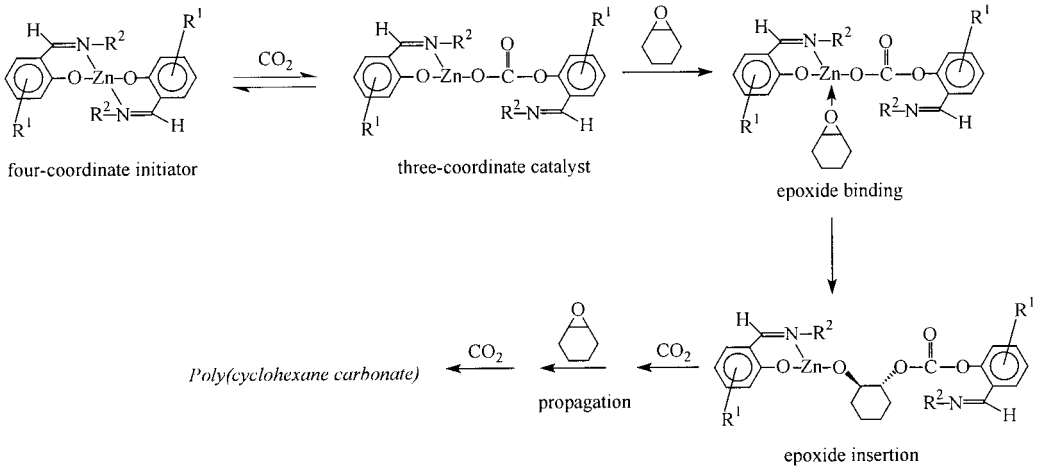

Table 3. Selected Bond Distances (Å) and Bond Angles (deg) for Complexes **4a**−**e**[a]

	Complex **4a**		
Zn−N(1)	1.990(3)	Zn−N(2)	1.998(3)
Zn−O(1)	1.925(3)	Zn−O(3)	1.925(2)
N(1)−C(12) (imine)	1.302(4)		
O(3)−Zn−O(1)	111.76(11)	N(2)−Zn−N(1)	128.77(12)
N(2)−Zn−O(3)	96.01(11)	N(2)−Zn−O(1)	109.44(12)
	Complex **4b**		
Zn−O(1)	1.908(3)	Zn−O(2)	1.924(3)
Zn−N(1)	1.997(3)	Zn−N(2)	1.984(3)
N(1)−C(1B) (imine)	1.295(5)		
O(2)−Zn−O(1)	105.59(12)	N(2)−Zn−N(1)	122.93(13)
N(2)−Zn−O(2)	96.38(12)	N(2)−Zn−O(1)	118.59(12)
	Complex **4c**		
Zn−O(1)	1.944(3)	Zn−O(2)	1.949(3)
Zn−N(1)	2.003(3)	Zn−N(2)	2.020(3)
N(1)−C(7) (imine)	1.287(5)		
O(2)−Zn−O(1)	112.37(11)	N(1)−Zn−N(2)	127.36(14)
O(2)−Zn−N(2)	93.90(12)	O(2)−Zn−N(1)	114.57(12)
	Complex **4d**		
Zn−O(1)	1.908(3)	Zn−O(2)	1.934(3)
Zn−N(1)	2.007(4)	Zn−N(2)	1.993(4)
N(1)−C(1) (imine)	1.300(6)		
O(1)−Zn−O(2)	112.56(15)	N(1)−Zn−N(2)	128.96(16)
O(2)−Zn−N(2)	113.18(15)	O(2)−Zn−N(1)	94.22(15)
	Complex **4e**		
Zn(1)−O(2)	1.958(3)	Zn(1)−N(2)	2.049(4)
Zn(1)−O(1)	2.022(3)	Zn(1)−N(1)	2.143(4)
N(2)−C(24) (imine)	1.309(6)	N(1)−C(8) (imine)	1.289(6)
O(1)−Zn(1)−O(2)	165.00(15)	O(1)−Zn(1)−N(2)	102.16(15)
O(1)−Zn(1)−N(1)	85.14(15)	O(1)−Zn(1)−O(1A)	76.75(15)
N(1)−Zn(1)−N(2)	110.54(16)	N(1)−Zn(1)−O(1A)	120.63(15)
N(2)−Zn(1)−O(1A)	128.34(15)	N(1)−Zn(1)−O(2)	92.64(16)
O(2)−Zn(1)−O(1A)	91.80(14)	N(2)−Zn(1)−O(2)	92.53(15)

[a] Estimated standard deviations in parentheses.

have increased as compared to the corresponding distances in the monomer complexes. The $O_{ax}-Zn-O_{ax}$ angle is 165.00(15)° and the equatorial angles are not far from 120° except for the $N_{eq}-Zn-N_{eq}$ angle which is 110.54(16)°, which can be contributed to the strain in the bridging ligands. The ^{1}H NMR spectrum of **4e** shows peaks that are slightly broadened, which could be a result of an equilibrium process between the dimeric and monomeric species in solution.

Although the bis(salicylaldiminato)zinc complexes were not the target species for serving as catalysts for the coupling of carbon dioxide and epoxides, it seemed plausible that these derivatives could be initiated by way of CO_2 insertion. This latter process does not require prior coordination of CO_2 to the metal center. Hence, in instances where the phenolic oxygen atom is not sterically encumbered, *reversible* CO_2 insertion into the Zn−O bond should occur with concomitant chelate ring-opening leading to an incipient three-coordinate zinc derivative. This process is represented in Scheme 2, where chelate ring-opening is driven in the presence of large quantities of CO_2 by formation of an eight-membered ring. Indeed, these four-coordinate complexes do exhibit varying activity for the co-polymerization of CO_2 and cyclohexene oxide. Their effectiveness for catalyzing this process spans a fairly broad range and appears to be influenced by the substituents on both the phenolic and ketimine rings.

The activities of these bis(salicylaldiminato)zinc complexes for catalyzing the alternating copolymerization of cyclohexene oxide and CO_2 to provide high molecular weight polycarbonates were investigated at 80 °C and 55 bar. The efficacy of these catalysts precursors decreased in the order **4a** > **4e** > **4b** > **4d** ≫ **4c**, with turnover frequencies (TOFs) = 15 > 7.3 > 5.0 > 1.2 > trace (g·polym/g·Zn/hr), respectively. The relatively high activity of **4a** can be attributed to the fact that the methyl group on the phenolic ring is both electron donating and not sterically hindering, thereby facilitating the insertion of CO_2. The remaining salicylaldiminato ligand on the three-coordinate catalyst formed for **4a** must not be, in this context, detrimental to the zinc center's ability to bind epoxides. It is important to note that there is a significant energy barrier to CO_2 insertion into the Zn−O bind due to the attendant disruption of the six-membered ring formed by the salicylaldminato ligand and the zinc center. Hence, the position of the equilibrium for formation of the putative three-coordinate zinc catalyst is strongly dependent on the nature of the Zn−O and Zn−N bonds. When these complexes are dissolved in C_6D_6 in an NMR tube and exposed to an atmosphere of $^{13}CO_2$ at ambient temperature, the only ^{13}C resonance observed was that of free $^{13}CO_2$ (125 ppm). Nevertheless, this barrier should be easily overcome under the conditions (80 °C and 55 bar) of catalysis. However, under *no* circumstances have we observed formation of significant quantities of the CO_2 insertion product. The three-coordinate zinc catalyst formed after CO_2 insertion is supported by the absence of polyether linkages within the polymer backbone as determined by ^{1}H NMR. In other words, all complexes in this study produced copolymer with >99% polycarbonate linkages similar to the three-coordinate $Zn(2,6\text{-}(tBu)_2OC_6H_3)_2(PCy_3)$

catalyst[2] and unlike the $Zn(2,6\text{-}(R)_2OC_6H_3)_2(solvent)_2$ complexes previously studied where the solvent ligands were labile.[1]

The decrease in catalytic activity in proceeding from the catalyst precursor **4a** to **4e** can be the net result of several contributing factors. First, if the difference in solid-state structures (*monomer* **4a** and *dimer* **4e**) exists in solution, dimer → monomer disruption is likely to impose an additional barrier to reaction. Furthermore, the presence of the electron-withdrawing CF_3 substituents in the 3 and 5 positions of the ketimine ring should inhibit CO_2 insertion into the Zn−O bond. On the other hand, it would be anticipated that these electron-withdrawing groups would enhance epoxide binding to the zinc center and thereby increase catalytic activity. Evidently, these various factors conspire leading to a decrease in catalytic activity in going from complex **4a** to **4e**. The reactivity difference between catalyst precursors **4a** and **4b** is more apparent. That is, the decline in catalytic activity in going from complex **4a** to **4b** most likely is the result of steric hindrance about the oxygen's lone pairs, thereby retarding the initiation step of CO_2 insertion. Further support for this steric argument can be seen by comparing the space filling models of complex **4a**, which has small methyl groups in the position ortho to the oxygen atom, and complex **4b**, which has larger tertiary butyl groups next to the oxygen atom. This comparison is shown in Figure 10 and best seen when viewed down the approximate C_{2v} axis between the oxygen atoms bound to the zinc center. Clearly shown in Figure 10 is the increase in steric bulk around the oxygen atoms on going from methyl substituents **A** and tertiary butyl substituents **B**.

Originally it was assumed that complex **4d** with the small, more electron releasing OMe substituent on the phenolate ligand would lead to an enhancement of catalytic activity by accelerating the CO_2 insertion process. Apparently, the concomitant decrease in epoxide binding leads to a net decrease in catalytic activity. By way of contrast, the electron-withdrawing chloride substituents in complex **4c**, which should retard CO_2 insertion and enhance epoxide binding, result in a greatly retarded catalytic system.

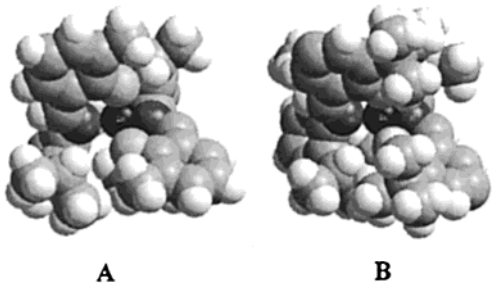

Figure 10. Space filling diagram of complex **4a** (**A**) and **4b** (**B**) showing the steric hindrance around the oxygen atom associated with an increase in steric bulk on going from methyl to tertiary butyl substituents.

Analysis of the formed poly(cyclohexane carbonate) by gel permeation chromatography shows that the polymer is rather polydispersed with Mn = 41 000 and Mw = 418 000. This high polydispersity of 10.3 most likely results from the fact that not all of the catalyst molecules are initiated at the same time resulting in polymer chains of various lengths. The fact that CO_2 does not readily insert into the Zn−O bonds of complexes **4a**−**e** supports this possibility.

Acknowledgment. Financial support from the National Science Foundation (CHE99-10342 and CHE 98-07975 for the purchase of X-ray equipment) and the Robert A. Welch Foundation is greatly appreciated.

Supporting Information Available: X-ray crystallographic files in CIF format for the structure determinations of **1a**, **c**, and **e** and **4a**−**e**. This material is available free of charge via the Internet at http://pubs.acs.org.

IC0006403